General Disclaimer

One or more of the Following Statements may affect this Document

- This document has been reproduced from the best copy furnished by the organizational source. It is being released in the interest of making available as much information as possible.

- This document may contain data, which exceeds the sheet parameters. It was furnished in this condition by the organizational source and is the best copy available.

- This document may contain tone-on-tone or color graphs, charts and/or pictures, which have been reproduced in black and white.

- This document is paginated as submitted by the original source.

- Portions of this document are not fully legible due to the historical nature of some of the material. However, it is the best reproduction available from the original submission.

DEVELOPMENT OF A SPECTROSCOPIC PHOTOELECTRIC IMAGING FABRY-PEROT INTERFEROMETER

PRELIMINARY OBSERVATIONAL RESULTS*

By

WM. HAYDEN SMITH† and JACK GELFAND†
Princeton University Observatory
Princeton, New Jersey 08540

ABSTRACT

In order to observe extended astronomical objects at high spatial and spectral resolution, we have constructed a spectroscopic photoelectric imaging Fabry-Perot interferometer (SPIFI). Among the properties chosen for the instrument are an air-spaced, piezoelectrically scanned design allowing an accurately settable free spectral range and employing a single etalon of high finesse. Careful design of the etalon mountings and optical train preserves high light throughput. We either obtain spectra of single spatial elements with a photomultiplier or use an SEC vidicon detector to record a series of images through the interferometer while scanning the wavelength in discrete steps. The latter procedure yields sufficient information to reconstruct spectral features over the entire object. For the conditions assumed, either series of observations requires only a small fraction of a rotational period for Jupiter or Saturn, for example. We have also constructed an electronic control system which permits rapid and flexible variation of the operational mode of the Fabry-Perot and its ancilliary devices so as to minimize loss of observational time. Finally, observational data are presented which demonstrate the degree to which we have achieved our design goals.

* This research is supported by Grant NGL 31-001-242 through the auspices of the National Aeronautics and Space Administration.

† Visiting Astronomers, Kitt Peak National Observatory, which is operated by the Association of Universities for Research in Astronomy, Inc. under contract with the National Science Foundation.

INTRODUCTION

In observational astronomy, studies of narrow wavelength regions at high resolving powers can often be conducted most profitably with Fabry-Perot interferometers (FPI). The particularly useful properties are its axial symmetry and its ability to accept light from a larger solid angle than dispersing spectrometers at equivalent resolving powers. These properties can be advantageous in all aspects of high resolution astronomical spectroscopy because atmospheric scintillations or "seeing" cause point objects to have finite diameters. However, it is especially applicable to objects with diameters considerably larger than a seeing element since it is possible to image the input object plane through the interferometer and then employing photoelectric detectors to rapidly and efficiently obtain spatial and spectral information. This paper describes the desired properties and the construction of such an FPI and shows some of the initial results acheived by its use.

Several FPIs for astronomical observations have been described in the literature. Most of these instruments are pressure-scanned. A well-known example is the PEPSIOS[1] which consists of three invar-spaced etalons. The relative plate spacings of the Pepsios' etalons must be rigidly controlled to superimpose the individual etalon transmission peaks. The spacings are therefore not easily and rapidly adjustable to arbitrary values. The enlarged free spectral achieved by the use of multiple etalons allows rather high resolving powers to be obtained by the PEPSIOS. Concommitantly, transmittance is reduced and can be seriously impaired by inter-etalon mismatches in transmittance. A low resolution triple etalon FPI has recently been constructed[2] where piezo-electric scanning and partial servo-loop stabilization are applied. Solid etalon filters have been designed for low

to medium resolution spectroscopic imagery of solar spatial structures.[3] The most interesting instrument recently described is the air-spaced servo-stabilized single etalon FPI of Hicks et al.[4] which has been applied to observational studies of planetary nebulae. This is a design which bears considerable similarity of purpose to our instrument.

Our interest is in the study of spatially extended sources, in particular the major planets, using an FPI with an imaging detector such as an SEC vidicon. We wish to study the spatial, spectral, and temporal variations of the absorptions due to the more abundant gases in the atmospheres of the major planets, i.e. H_2, CH_4, and NH_3. The transitions of major interest lie almost entirely in the wavelength region between 4000 Å and 10000 Å, where detectors of high quantum efficiency are available. Quantum detectors are required since even bright objects such as Jupiter provide quite low fluxes when divided up into many spatial elements at high spectral resolving powers. Further, since we wish to determine the existence of temporal variations, only a very limited time can be consumed in obtaining spectra of high signal-to-noise, especially in rapidly rotating objects such as Jupiter and Saturn. Finally, it is of considerable importance to obtain spectra of sufficiently high spectral resolution to accurately define the center-to-limb variation (CTL) of the equivalent widths of weak transitions (a few mÅ) and to define line profiles, if possible. Calculations in this observatory based upon inhomogeneous cloud models for Jupiter show that such variations may be only 10-20%. Therefore, for weak transitions such as the H_2 4-0 quadrupole transition at 6368 Å ($W_e \sim 9$ mÅ), accurate determination of the CTL variation requires a very high signal-to-noise ratio (S/N) be achieved in the observational data.

INSTRUMENTAL DESIGN CONSIDERATIONS

The above considerations place severe constraints on the FPI's design, and demand certain compromises be reached in its capabilities. First, the observational circumstances do not allow the full resolving powers attainable by multiple FPI's to be utilized. Atmospheric scintillations generally limit the "seeing" to about 2 seconds of arc for ground-based observations,[5] other than greatly exceptional circumstances. A rapidly rotating planet such as Jupiter or Saturn then will suffer a mixing of Doppler-shifted spectral elements from different portions of the planet within the seeing disc. This effects limits the spectral resolution at 6368 Å to 0.025 Å for Jupiter or to 0.042 Å for Saturn for 2" seeing. Guidance errors will tend to further reduce the attainable resolution.

Observations[6] in the visible and near-infrared show that H_2, CH_4, and NH_3 are among the most abundant gases present in the atmospheres of the major planets. The line formation problem for the H_2 quadrupolar transitions have been discussed by Fink and Belton.[7] The collision narrowing, in spite of a pressure shift,[8] produces a line narrower than the seeing resolution limit, thereby not permitting the direct measurement of a line profile for these transitions under likely conditions of seeing. The line formation for CH_4 and NH_3 occurs at levels such that the intrinsic line widths are greater than that due to seeing effects so that line profiles may, in principle, be obtained. For example, Mason[9] has reported line widths of about 0.2 Å for the 6450 Å band of NH_3 observed in Jupiter. The line formation is such then that H_2 quadrupolar transition observations are limited by the seeing, while line profiles for the CH_4 and NH_3 bands in the 6000-7000 Å region can be obtained at spectral resolutions of about 0.1 Å. Poorer seeing can restrict the useful resolving powers even further.

Finally, the considerations of the available flux per spatial element (with TV camera, per pixel) and the concommittant time required to integrate to a desired signal-to-noise will limit some choices of the instrumental parameters. Considering Jupiter as an example, we calculate that, near opposition when Jupiter has a visual magnitude of -2.5 and an angular diameter of approximately 45", a total of approximately 140,000 photons per second per 100 mÅ should be detected for the entire disc when observing with the SPIFI, assuming that we are collecting light with a 1.52 meter telescope, and that each optical element has an assumed efficiency as listed in Table I. The flux from a 2" spatial element should result in about 350 detected photoelectrons, on the average for the limb-darkened disc. There should be about a factor of five variation from the center of the disc to the limb, lengthening the time of observation at constant S/N as the limb is approached. In this example, the scan across the line, including ten half widths about the line center, will require about ten minutes to achieve a S/N of 100 near the center of the disc. Since Saturn is about a factor of four lower in surface brightness than Jupiter, the flux will be correspondingly reduced, per spatial element of 2 arc-seconds. On a typical night, we can expect to observe consecutively a minimum of 15 spatial elements for Jupiter using an available photomultiplier such as the RCA C31034 A, even if all observed elements were placed near a limb. This data acquisition rate is a dramatic improvement over conventional spectroscopic techniques. Although comparisons are difficult to make, Bergstrahl, for example, obtained a similar sequence of observations in the $3\nu_3$ methane band on Jupiter which usually required a night's observation per spatial point, obviating the possibility of observing short term spectral or spatial variations.

This section of the design considerations points up the advantages of two dimensional photoelectric detectors such as the SEC vidicon, when used in conjunction

with an FPI to obtain monochromatic images of extended objects such as Jupiter and Saturn. For the parameters considered and replacing the photomultiplier with the SEC vidicon, a total exposure of less than one hour should allow the accumulation of 15 images of Jupiter in a 0.1 Å band pass. Each image will contain more than 400 spatial elements of 2" with a S/N of at least 40/1 for the lowest brightness element. This estimate follows from the known properties of the SEC vidicon as determined by the Princeton TV group.[11] Such complete spatial information at the indicated spectral resolving power would require prohibitive amounts of telescope time with conventional methods, and would completely convolve any spatial and temporal variations occuring within the lengthy period required for the spectral observations.

The television sensor retains the major advantages of photographic film, but has more than ten times the effective quantum efficiency, and high photometric accuracy. Basically, this camera allows the integration of a light signal by accumulating secondary electrons produced in a KCl frit by accelerated photoelectrons from the photocathode. The SEC vidicon has a secondary electron multiplication of about seventy. This stored charge is read out via a scanning electron beam and recorded in analogue form on magnetic tape along with location information to determine from which portion of the photocathode the photoelectron was emitted. In this manner, digital images of high photometric accuracy may be reconstructed. Integration times of several hours are possible with this low noise device before serious loss of dynamic range occurs. Since for the conditions described, the planetary image at f/60 for Jupiter is only about 3.0 mm in diameter, we would be able to more efficiently use the 25 x 25 mm format of the TV camera if we arranged to move the image over the storage frit of the camera for each sequential wavelength

to be imaged. A magnetic deflection coil has been added to the photoelectron imaging section of the TV camera to accomplish this purpose.

FABRY-PEROT INTERFEROMETRY: GENERAL CONSIDERATIONS

The FPI is a classical spectroscopic instrument that has recently undergone a revival in popularity due to technological advances in figuring etalons, producing high reflectance, low loss dielectric coatings, and in the advent of piezoelectric elements for FPI scanning. A recent discussion of some of these advances and methods has recently been given by Roesler.[12]

The transmission function of a FPI consists of a series of peaks at each integral number of half wavelengths (or order of phase delay between the etalon mirrors). An ideal FPI can be represented by a Dirac comb, III $(\psi/2\pi)$, where ψ is the phase delay.[13] Given in terms of the geometry of the air-spaced FPI.

$$\psi = 4\pi \ell \sigma \cos \theta \qquad (1)$$

where ℓ, σ, and θ are the distance between the plates in cm., the wavenumber of the incident light in cm^{-1}, and θ is the angle of incident light rays with respect to the normal to the FPI plates, respectively. The pass band of a practical FPI is given by the convolution of a Dirac comb with a series of broadening functions representing width contributions of the plate reflectivity, surface figure, and entrance aperture size. The finesse is defined as the ratio of the interorder separation of the transmission maxima to their full widths at half maximum.

It is necessary to isolate the transmission passband of a single order of the FPI in order to use it as a spectrometer. Available multi-cavity dielectric

filters allow a single etalon to be blocked so as to obtain medium-to-high resolving powers. We have chosen to use a Burleigh Instruments Model RC-50 FPI as the primary element of our instrument. With this instrument, we have obtained a finesse of over 75 by use of $\lambda/200$ etalon plates with 97% reflective coatings with a useful plate area of about 45 mm diameter. Careful mounting techniques allow the maintenance of the $\lambda/200$ figure, and thereby a transmittance of more than 90% for the FPI. The blocking filters used to date are three cavity filters of 3 to 4 Ångstroms full width at half maximum (Spectro-Film Inc.) These filters have peak transmittances of 30 to 40%. A separate filter is employed for each wavelength interval to be investigated. An interval of up to 30 Å can be scanned by tilting the filter up to 15°. The wavelength scans to the blue without serious degradation of the filter profile.

A FPI with a finesse of 75, blocked by a three period filter of 3.5 Å half-width, can be used at spectral resolving powers of over 80,000 with much less than 1% parasitic light for a scanning range of more than 3 Å.[14] Parasitic light results from the incomplete suppression of other orders of the FPI by the blocking filter. This high spectral resolving power is adequate for the observations contemplated for this instrument, as described above. Higher resolving powers can be obtained at the expense of a larger amount of parasitic light or a reduced scanning range. Since we have a very accurate method for determining the parasitic light,[15] this option will sometimes be exercised when the increased resolving power is useful.

There are many possible configurations for imaging through an FPI-filter system.[16-18] In this instrument, an image of the planet is formed at an entrance aperture and the rays from each image point are collimated by a plano-convex lens. Both the filter and the FPI are placed in the collimated section. The light is reimaged by another plano-convex lens through an exit aperture. The exit and entrance apertures eliminate ghost images formed by extraneous reflections from

the etalon and filter surfaces. The spectral response of the FPI across this entrance aperture from equation 1 is

$$\lambda(\theta) = \lambda(0) \cos\theta \qquad (2)$$

where $\lambda(0)$ is the wavelength of normal incidence, and $\lambda(\theta)$ is the wavelength of the peak spectral response for an image point whose collimated rays are at an angle θ to the FPI axis.

INSTRUMENT CONSTRUCTION AND OPERATION

Our design considerations are influenced by the intention to be able to use the FPI at any telescope focal position, particularly at the Cassegrainian focus. This requires that the instrument be very stable mechanically so as to not be influenced by the telescope movement and thermally controlled to be insensitive to changes in the ambient temperature. The requirement for the FPI stability is also dependent upon the time interval required for an observational sequence to be completed, by the ease of calibration, and by methods which may be developed for reducing the thermal, electronic, and mechanical perturbations on the FPI encountered in the operating environment. In order to satisfy as many of these criteria as possible, we have built the FPI and its associated optical system onto a magnesium I-beam optical bench enclosed within an insulated aluminum housing with interchangeable side doors for easy access. This arrangement provides a very rigid enclosure for the several configurations of the FPI and the optical element, e.g., for the TV mode or the PMT mode. Both the outer walls and the inner aluminum box containing the FPI and the blocking filter are thermally controlled by

a multi-channel thermostatting system capable of maintaining better than 0.1°C temperature stability within the inner box over a wide range of external conditions.

An FPI must be provided with a group of ancilliary devices for its practical use. These include a provision for a reference channel to remove atmospheric transparency variations, calibration lamps with appropriate emission lines, a continuum source for measurement of the filter profiles and for calibration of the TV response over its active imaging area, a variety of Fabry-Perot input and exit apertures and means of off-axis guiding. These elements must be frequently interchanged during a night's observations and thus must be mounted in a fashion that allows their rapid and accurate placement on the optical axis by remote control, both for convenience and to preserve a stable thermal environment.

A schematic of the component placement in the instrument is shown in Figure 1. The telescope image is focussed at the entrance aperture of the instrument. A guider is provided which reflects the off-axis light to an eyepiece. Guidance may then be accomplished by the use of a reference object in the telescope field. A dichroic beam-splitter may also be used so that the planetary image itself provides the light for guidance. A field lens at the primary image focus directs the rays to a reimaging lens by imaging the telescope primary in the plane of the reimaging lens. The reimaging lens transfers the primary focus image to the FPI input aperture and adjusts the size of image to be compatible with the spectral resolution of the FPI. The emission line and calibration lamps are provided at this point. The sources and reimaging lenses along with various-sized pinhole input apertures are mounted on Geneva mechanisms. These devices place the chosen element onto the optical axis by a rotary motion. The device is driven by dc motors. Binary coded light emitting diodes and sensors operating in the infrared indicate which aperture and entrance element are in position. After the entrance

aperture, a dual beamsplitter consisting of two beamsplitter cubes cemented together directs 2% of the light to a reference photomultiplier and 2% to an eyepiece to allow observation of the light transmitted by the pinhole for fine guidance and alignment purposes. The focal position of a collimating lens is placed at the entrance pinhole, and the FPI and blocking filter are placed in the resulting collimated section. Reimaging and transfer lenses then form images of the proper size upon the SEC vidicon photocathode or on the PMT photocathode (RCA 31034A).

The size of the image on the photocathode depends upon the spatial resolution to be attained for the object being observed, and upon the signal-to-noise and modulation transfer characteristics of the SEC vidicon. We chose to use 100-200 micron pixels which will produce an optimum S/N of about 40/1 for our exposure of 3000 photoelectrons per pixel. The photoelectrons emitted in response to the incident photons are focussed on a selected spot of the KCl storage frit by the magnetic deflection system. This spot is displaced to produce a sequence of images which are incremented in wavelength by stepping the FPI plate spacing. Subsequently, the images are read out onto magnetic tape for computer processing.

The mechanical portions of the FPI are operated through an electronic control system designed especially to meet the present observational objectives. A schematic representation of the control system, which we have dubbed the DASS as an acronym for Data Acquisition Sub-System (recognizing that it is a Swedish word), is shown in Figure 2. This system provides two channels for pulse counting from the reference and data PMT's. The count accumulated in the data channel depends upon either a time base which can be preset for an arbitrary integration period or upon the accumulation of counts in the reference channel to a predetermined number. The reference channel PMT is illuminated by the 2% of the incident light reflected by

the prism beam splitter, and passing a broad band filter. The count rate in this channel is adjusted to be at least five and usually ten times that of the data channel, and compensates for variations in the atmospheric transparency during an integration of an observational data point. The DASS contains a clock for the accurate timing of each integration interval, and for providing the correct UT for each observation. The cycle is begun by establishing where within the spectral interval we wish to start the integration. This position is set upon a digital switch which corresponds to a certain voltage on a d/a converter which drives the high voltage ramp for scanning the pz elements of the FPI. The integration proceeds according to the timing interval or the reference channel count required. At the end of the integration, the data channel, the Universal Time , and the digital ramp position are read onto a magnetic tape. Then, a new cycle is initiated by the incrementing of the ramp, and the recording of a new UT as the integration begins again. Each spectral scan, whether with a PMT or the TV camera, requires a particular set of pin holes depending upon the spectral and spatial resolution to be attained. These are rotated into place by observing digital readouts on the instrument panel which correspond to the desired element. Either the off-axis guider or the behind-the-pin-hole guider is used to provide fine corrections in the main telescope tracking to maintain the accurate pointing of the telescope during the integration period. Before and after the integration, a scan of a reference line from a hollow cathode lamp provides the information to calibrate the wavelength and determine whether any substantial drifts or misalignements occurred during the integration period. The white light is then rotated into the optical axis for a very accurate scan of the filter profile to be divided out during data analysis. Lunar scans provide a measurement of the influence of terrestrial absorptions, air mass, and the solar absorption spectrum. When using the TV system, the incrementation

of the ramp to the pz elements which scan the FPI also causes an incrementation of TV deflection system to place the planetary image onto a new portion of the storage frit of the TV camera. The thermal control system for the FPI is automatic and does not require any attention during the course of a night's observations. The filter tilt is, at present, manually adjusted with the use of an appropriate reference line from the hollow cathode lamp to pass the desired wavelength at the maximum of the pass band. The complete system, as presently constituted, requires three people for its operation in the TV mode, and two in the PMT mode.

We have used this apparatus in two very different operating conditions, to date. We have attached the SPIFI to the Cassegrainian focus of our 36" telescope here in Princeton for the initial tests. This environment requires that the FPI be insensitive to changes in temperature and in attitude of the telescope. We found that the thermal stabilization worked well in spite of rather large changes in the ambient temperature. The major problem encountered was the effect of the telescope motion on the alignment of the FPI. The variation in the orientation of the FPI produced a gradual misalignment over about a thirty minute period, as determined by test scans of Fraunhofer Lines in the reflected Solar spectrum from the Lunar surface. Each scan required less than one minute for a 5" section of the moon to achieve a S/N of greater than 300/1. We also found that if we rotated the FPI on the bearing race at the Cassegrainian focus, so that the vertical axis remained vertical during the observational period, much of the misalignment effect was removed. This misalignment may arise partially from the fact that the FPI is not supported other than in a vertical direction, however, a complete solution to this source of misalignment requires more than an improved support. This will be discussed later in this paper.

We were granted observational time at the McMath Solar observatory to use the Coude-like focus there. In this position, our instrument is not subject to any varying gravitational forces during the course of the observations, and only to modest temperature variations. Our FPI was fitted with a set of plates to allow a finesse of more than 75. In Figure 3, a scan of the KrI reference line is presented to illustrate the finesse obtained. From this line scan we find that we are reaching a resolving power of 60,000 at a finesse of 65, with a parasitic light much less than 1%, for a scan range of more than 3 Å. Once the SPIFI was thermally in equilibrium, alignment was often stable for several days, apart from small axial movements ($\sim \pm 0.05$ Å). With these instrumental parameters, we then scanned absorption lines arising from the H_2 quadrupolar transition 4-0 S(1) at 6368.76 Å (lab) in both Jupiter and Saturn, and subsequently observed the NH_3 $5\nu_1$ transition at 6457.2 Å, both with the PMT. The H_2 transition on Jupiter is shown in Figure 4, where the absorption line's Doppler shift from the center of the disc to the limb is demonstrated. This observation was made with seeing of approximately 2-3" and a corresponding pin hole. The line shifts to the red as we observe a portion of the planet moving away from us. The shift increases linearly with CTL position to a maximum of 0.26 Å at our spatial resolution. A similar observation of Saturn is shown in Figure 6, although the spatial variation can be less well resolved because of the small apparent diameter of Saturn. In both cases, the lines show an equivalent width near 9 mÅ at the disc center, increasing toward the limb for Jupiter. The detailed analysis of these observations is now being carried out here in the laboratory.

In Figure 6, we present a scan of the NH_3 transition at 6457.2 Å, along with two adjacent solar Fraunhofer lines. This line is seen to have a half width greater

than the instrumental half width as can be seen by comparison with the adjacent solar lines. This line is considerably stronger than the H_2 transition, having an equivalent width of more than 50 mÅ. For this reason, we decided to make our first observations of Jupiter with the TV camera at the wavelength of this absorption line.

The TV observations of Jupiter were carried out in the same manner as the PMT, with the exception that the reference line scans to determine whether the FPI has been stable during image acquisition, can be made only after the entire exposure. Generally, we were successful in that the FPI stability was adequate for this purpose. A sample of the TV data is shown in Figure 7. The image format is that described above. There is a solar Fraunhofer line in the pass band of the FPI so that a diffuse vertical band appears across the disc of Jupiter going from North to South. The position of the line, which is Fe II 6456.4 Å, shifts as the FPI pass band is incremented. The FPI wavelength increment scans toward the blue so that the band on the planet is seen to shift toward the blue-shifted limb during the observation. We note that the S/N available in this photographic display of our data can not adequately represent the actual data, but in any case, the absorption feature is clearly visible in the photograph. The data indicate that the observational program was in fact successful in that TV images with good spatial and high spectral resolution were obtained with our FPI. The lack of the usual banded appearance of Jupiter is partially due to the following factors. First, the contrast in those features is very low in the red. Secondly, the exposures here are long compared with the usual pictures shown of Jupiter. Consequently, the measured seeing of 4-5" considerably blurs the images. A close examination of the data shows the expected banded structure so that, in fact, the images

were in reasonably good focus. Detailed reduction and analysis of these data are in progress.

The quality of the focus is better demonstrated by a TV image taken of Saturn at the same wavelength as for Jupiter. We made PMT observations of the NH_3 region for Saturn, and found that the NH_3 was undetectable at our sensitivity level. We therefore made single wavelength exposures for Saturn rather than scans in wavelength. The exposures were about thirty seconds in length. Figure 8 shows one of the resultant photographs. Seeing during the exposure was about 4" so that across the disc we could expect only four or five resolved spatial elements. It is easy to see that we achieved this spatial resolution. The separation between the rings and the planet is about 5", and is well resolved.

The above results give us the assurance that the major goals of this observational program are in fact attainable and that our FPI design is well-conceived. There are several areas in which improvements are being made to optimize the stability of the FPI and the usage we make of the telescope time available to us for our observations. Most important to the development of the astronomical FPI at present is the addition of a method of active stabilization which can correct for moderate misalignments due to the inevitable mechanical and electrical instabilities of an air-spaced Fabry-Perot. The instability that is the most difficult to correct is the type found when we operated at the Cassegrainian focus, and which is due to minute mechanical relaxations in the FPI occurring because of the movement of the telescope as it tracks an object across the sky. Although we found it possible to make observations for as much as one hour by rotating the instrument on the bearing at the Cass position, this time interval is not sufficient for many observations, and introduces a systematic error in the wavelength calibration of the FPI.

Other sources of instability include instabilities in the electronics which drive the pz elements, and temperature effects. Both these sources of drift can relatively easily be controlled to within acceptable limits.

The servo-stabilized FPI described by Hicks et al.[4] is an ideal solution to problems of all these types of instabilities, if they can be constrained to produce drifts or misalignments which are correctable by the pz elements. This condition is already satisfied by our instrument without a stabilization system. Thus, we are now constructing a servo-stabilizing system similar to that of Hicks et al.[4]

The other area in which an improvement in technique will prove valuable is automatic fine guidance. Many of our observational interests require that an object, or a portion of it, remain at a fixed position within our optical system, i.e. accurately placed upon the center of the photocathode of the TV camera, for a considerable period of time. Manual fine guidance leaves much to be desired in achieving this goal. A real time servo-system, possibly of the type described by Hunten,[19] can provide this fine guidance since,by stabilizing the mean position of the image, such a device performs the fine guidance function. In addition, it performs this guidance in a manner producing an easily definable guidance error. This will allow us to determine the portion of the resultant image blurring that is a result of our guidance errors, an important result. More sophisticated systems are possible[20] in which the mean position of the image is stabilized, and the image itself is corrected for atmospheric effects which result in the seeing. Such a system is presently under test by a group of scientists at the Bell Telephone Laboratory,[21] and has already shown positive results in the laboratory. One form of such fine guidance will be added to our system, probably an image stabilizer at first, then the more sophisticated "seeing corrector" when such systems have proven themselves to be feasible.

The application of this method to the observation of HII regions has also been begun. Easily measurable fluxes at H_α have been observed with considerable spatial and radial velocity structure for the Lagoon Nebula. We are preparing for observations in the near ultraviolet where single etalon Fabry-Perots blocked by interference filters gain their greatest advantages with regard to effective throughput. In this region, the use of acousto-optic filters[22] as blocking elements may offer very significant advantages. The charge-coupled device now available at Princeton University Observatory[23] will be used as an area detector in place of the SEC vidicon in future observations, primarily because of a superior quantum efficiency and dynamic range.

Table 1. Computation of Expected Flux from Jupiter

The following parameters are assumed:

$M_V(4) = -2.5$;

diameter on sky: 45 arc-sec

atmospheric transparency 0.80 @ 6000 Å

Telescope: 1.52 m. unobscured, efficiency 0.75

Optical Transfer System: efficiency 0.75

FPI Transmittance: 0.65

Blocking Filter Transmittance: 0.30

Photomultiplier Quantum Efficiency: 0.05

Instrumental transmission halfwidth: 100 mÅ

Spatial Element on Jupiter: $(2 \text{ arc sec})^2$

References

1. Mook, J.E., McNutt, Roesler, F.L., and Chabbal, R., Appl. Optics, 9, 873 (1963).
2. Drummond, D. and Gallagher, A., Rev. Sci. Inst. 44, 396 (1973).
3. Title, A.M., Harvard College Observatory Report TR-20 (1971).
4. Hicks, T.R., Reay, N.K., and Scaddan, R.J., J. Phys. E: Sci. Inst. 7, 27 (1974).
5. King, I.R., Pub. Astron. Soc. Pacif. 83, 199 (1971).
6. Hunten, D.M., Space Sci. Rev. 12, 539 (1971).
7. Fink, U. and Belton, M.J.S., J. Atm. Sci., 26, 952 (1969).
8. McKellar, A.R.W., preprint, 1975.
9. Mason, H.P., Astrophys. Space Sci., 7, 424 (1970).
10. Bergstrahl, J.T., Icarus, 19, 390 (1973).
11. Zucchino, P., 6th Symposium of Photoelectronic Image Devices (September 1974).
12. Roesler, F.L., Methods of Experimental Physics, Vol. 12, Chpt. 12, pp. 531-569, Ed. Carleton, Academic Press (1974).
13. Steel, W.H., Interferometry (Oxford Press, 1967).
14. Title, A.M., Harvard College Observatory Report TR-18/
15. Smith, W.H., Gelfand, J. and Larach, D., "An Accurate Method for Determination of Parasitic Light Levels in Fabry-Perot Interferometers", in preparation.
16. Courtes, G., Vistas in Astronomy, Vol. 14, Pergamon Press (1972).
17. Sheglov, P. IAU Symposium #34, Planetary Nebulae, pp. 270-272 (1968).
18. Meaburn, J. Applied Optics, 14, 465 (1975).
19. Hunten, D.M., Methods of Experimental Physics., Vol. 12, Chpt. 4, pp. 193-219, Academic Press (1974).
20. Dyson, F., Preprints (1974).
21. Brown, T., private communication.
22. Isomet Corp., Oakland, New Jersey.
23. Renda, G., and Lowrance, J.L., Proceedings JPL Conference on CCD Imagery, March (1975)

Figure Captions

Figure 1. Layout of the optical system of the SPIFI indicating the positions of all components.

Figure 2. Schematic of the electronic system used in scanning the SPIFI, and in data acquisition.

Figure 3. Scan of the Kr I 6373 Å doublet to illustrate the finesse achieved under observational conditions($\mathfrak{F} = 65$).

Figure 4. Tracings of single scans of the H_2 4-0 S(1) line on Jupiter for five positions from the disc center to the extreme red(R) limb.

Figure 5. Tracings of single scans as above, except for Saturn and with the indicated positions being observed. The filter profile is indicated.

Figure 6. Tracing of the NH_3 6457.2 Å line on Jupiter, disc center, along with two Fraunhofer lines. The width of the NH_3 feature is greater than the instrumental profile width. The two weaker features are also real. The filter profile is indicated.

Figure 7. Television frame showing a series of images of Jupiter. The Solar Fe II 6456.4 Å Fraunhofer line is seen as a slanted line traversing the planetary disc. In the last three frames, the Ca I 6455.6 Å line is seen to begin its traversing of the disc as the SPIFI is scanned.

Figure 8. Television frame of Saturn at 6457.2 Å in the continuum. This frame illustrates the spatial resolution achieved to be at least 5" from the disc-ring separation.

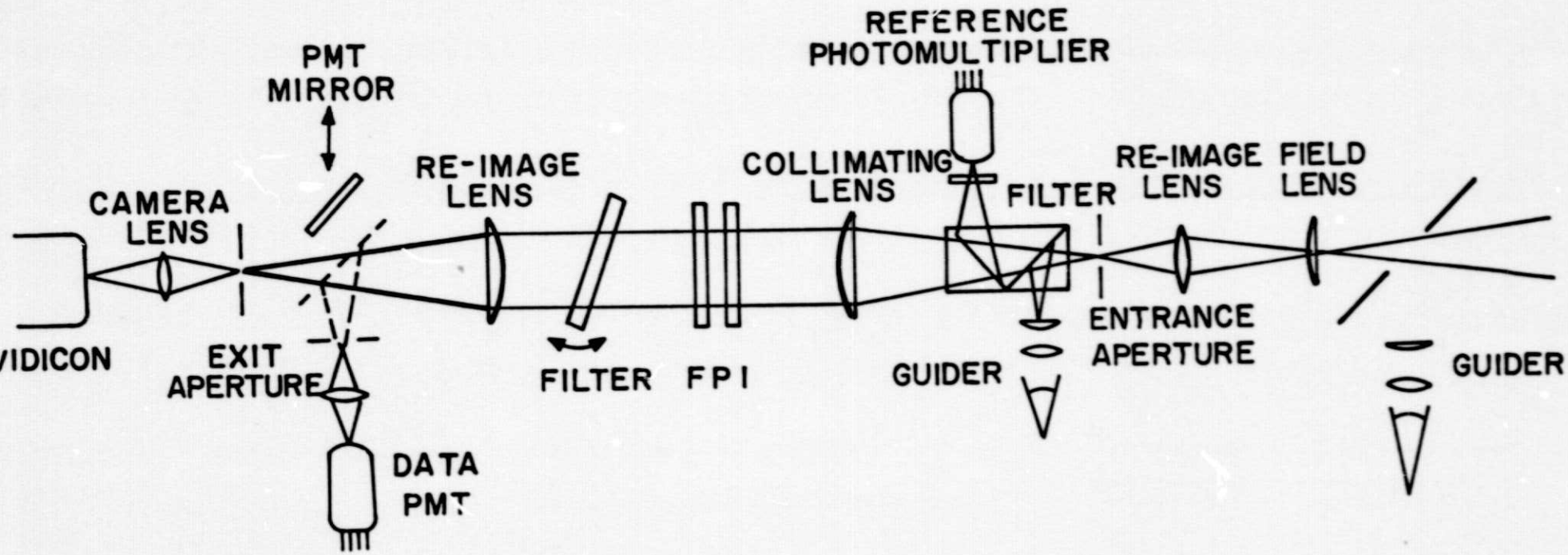
PMT
MIRROR
REFERENCE
PHOTOMULTIPLIER
CAMERA
LENS
RE-IMAGE
LENS
COLLIMATING
LENS
FILTER
RE-IMAGE
LENS
FIELD
LENS
VIDICON
EXIT
APERTURE
FILTER
FPI
GUIDER
ENTRANCE
APERTURE
GUIDER
DATA
PMT

PLANETARY IMAGING INTERFEROMETER
DATA AND CONTROL CIRCUITRY

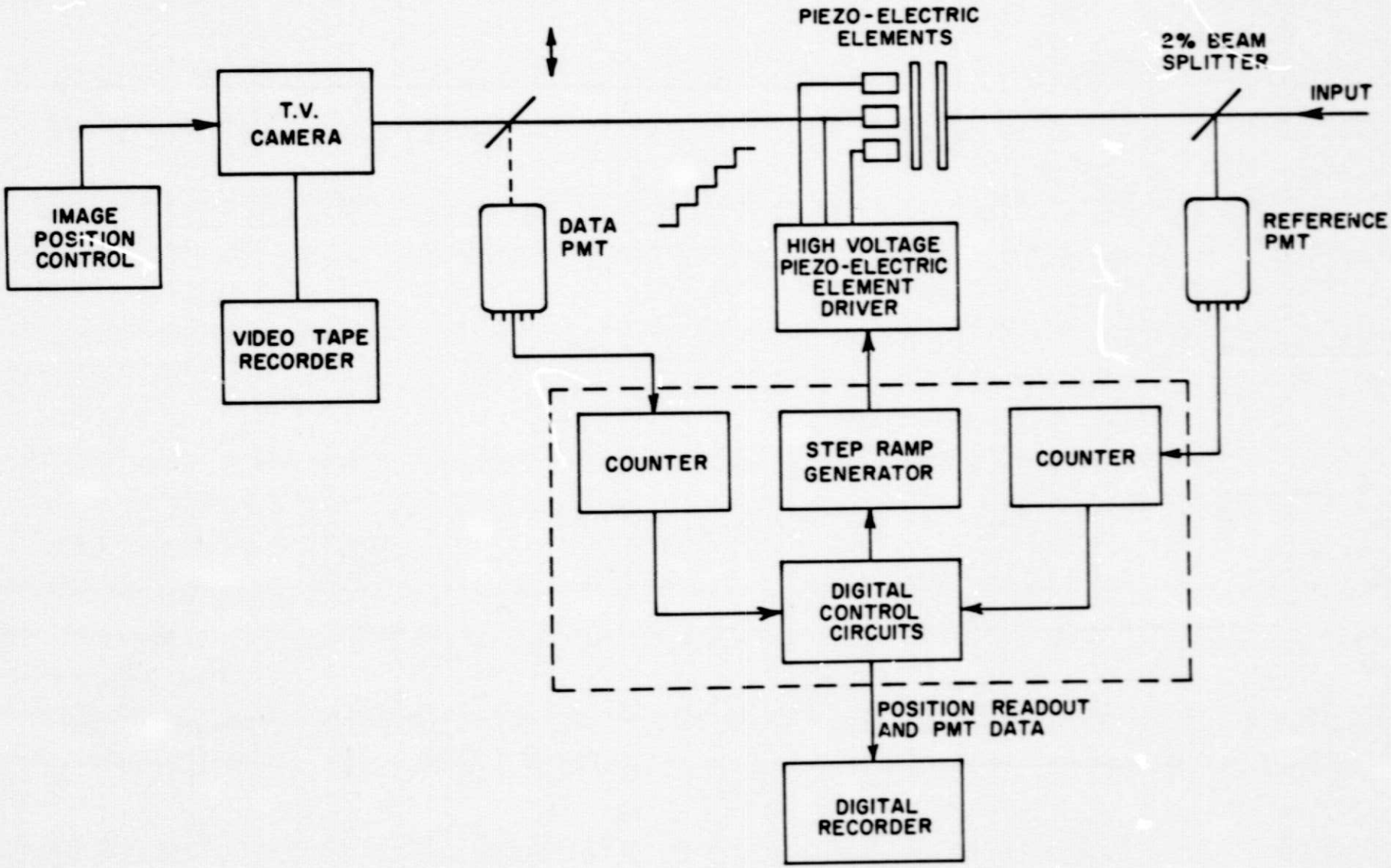

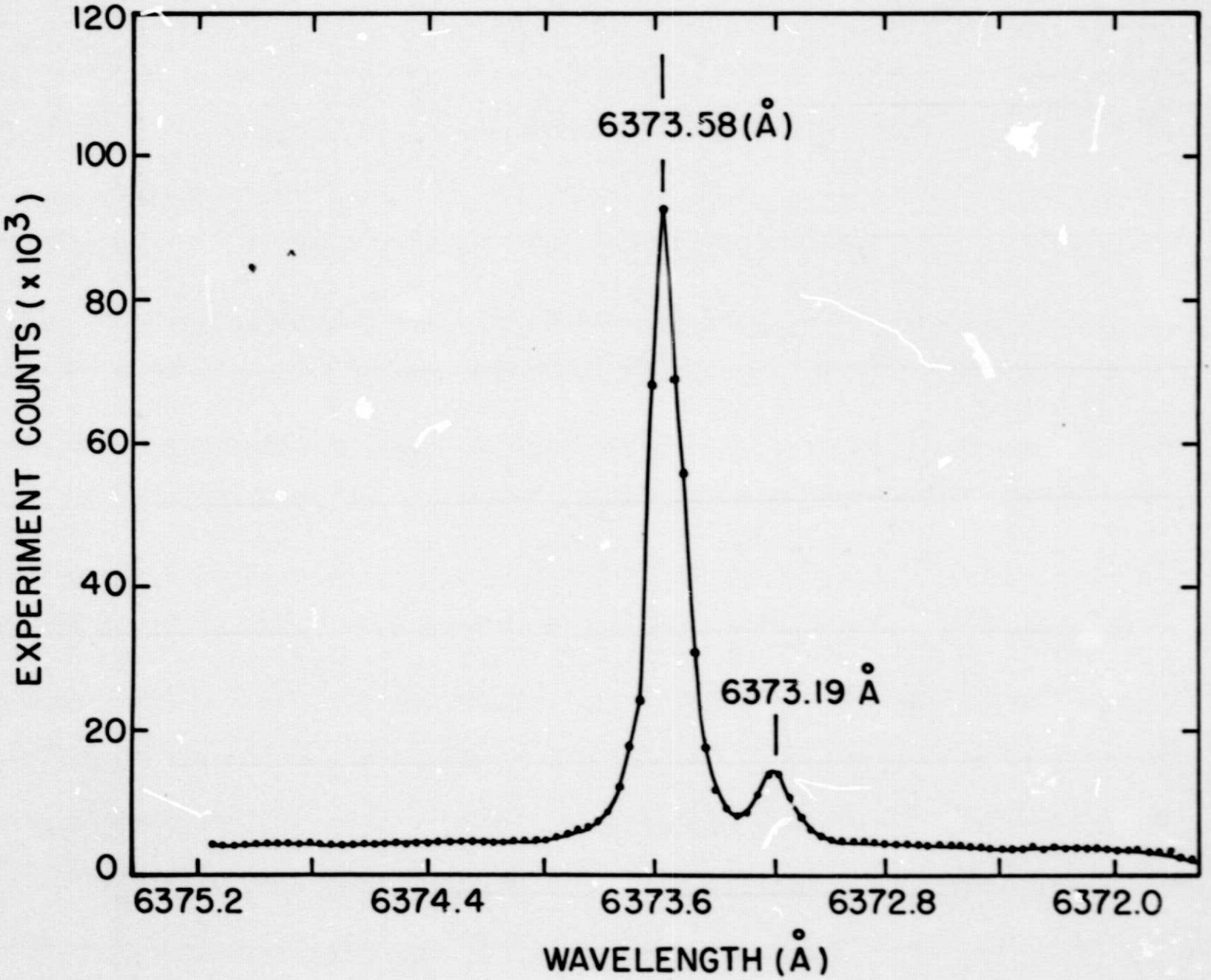
120
100
80
60
40
20
0
EXPERIMENT COUNTS (x 10³)
6373.58(Å)
6373.19 Å
6375.2
6374.4
6373.6
6372.8
6372.0
WAVELENGTH (Å)

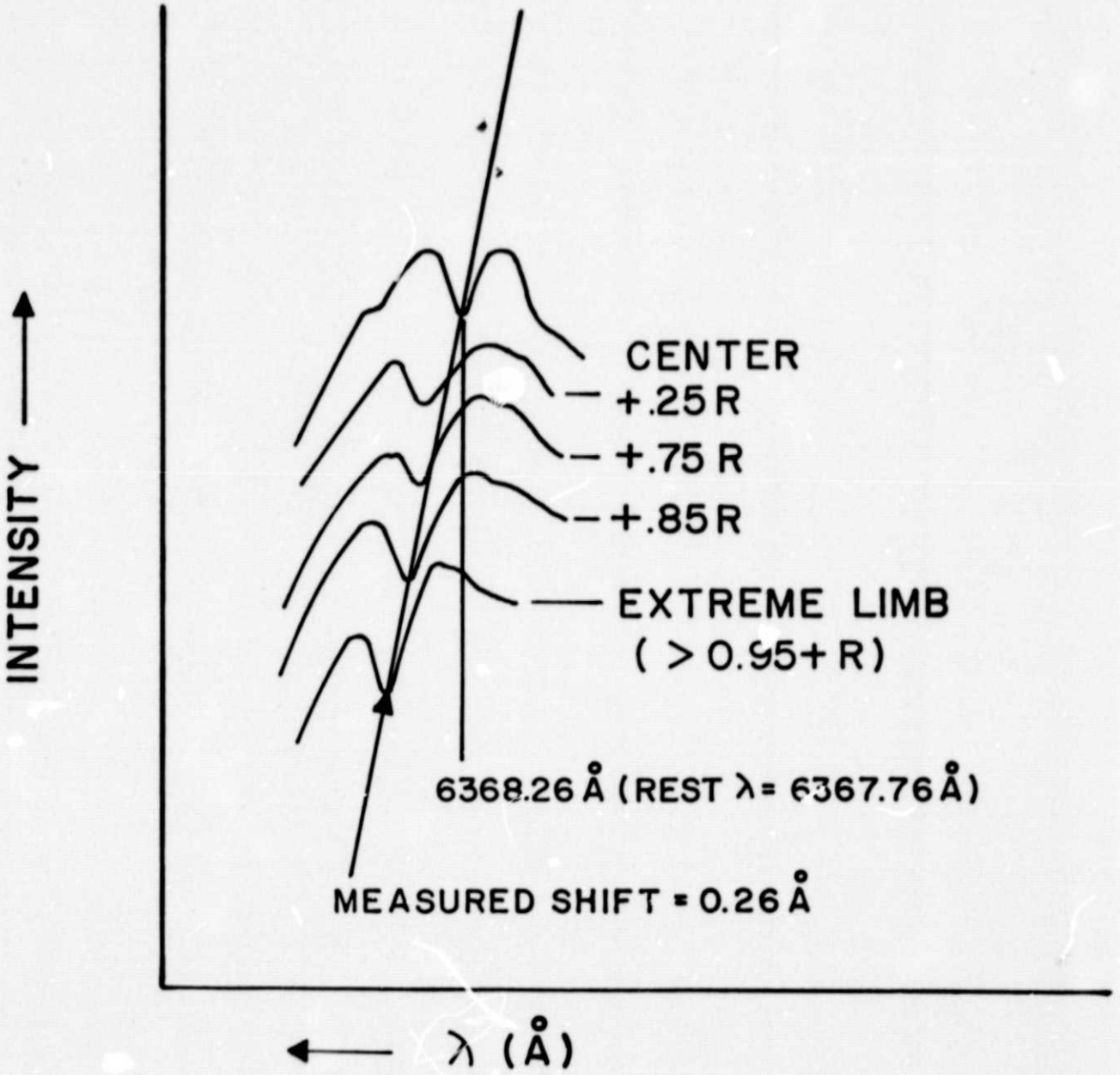
INTENSITY
CENTER
+.25 R
+.75 R
+.85 R
EXTREME LIMB
(> 0.95+ R)
6368.26 Å (REST λ = 6367.76 Å)
MEASURED SHIFT = 0.26 Å
λ (Å)

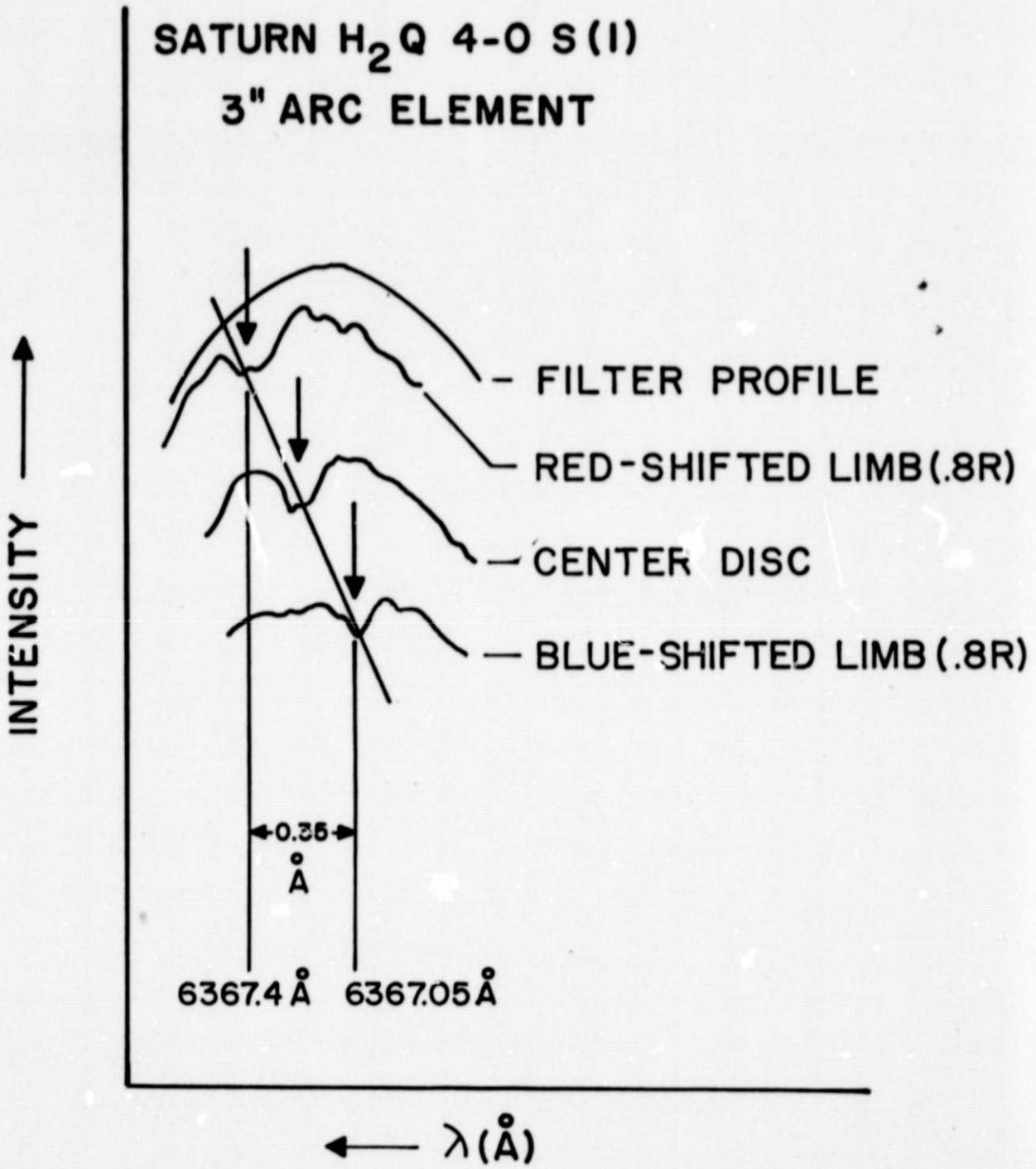
SATURN H_2Q 4-0 S(I)
3" ARC ELEMENT
INTENSITY
FILTER PROFILE
RED-SHIFTED LIMB(.8R)
CENTER DISC
BLUE-SHIFTED LIMB(.8R)
0.35 Å
6367.4 Å
6367.05 Å
λ(Å)

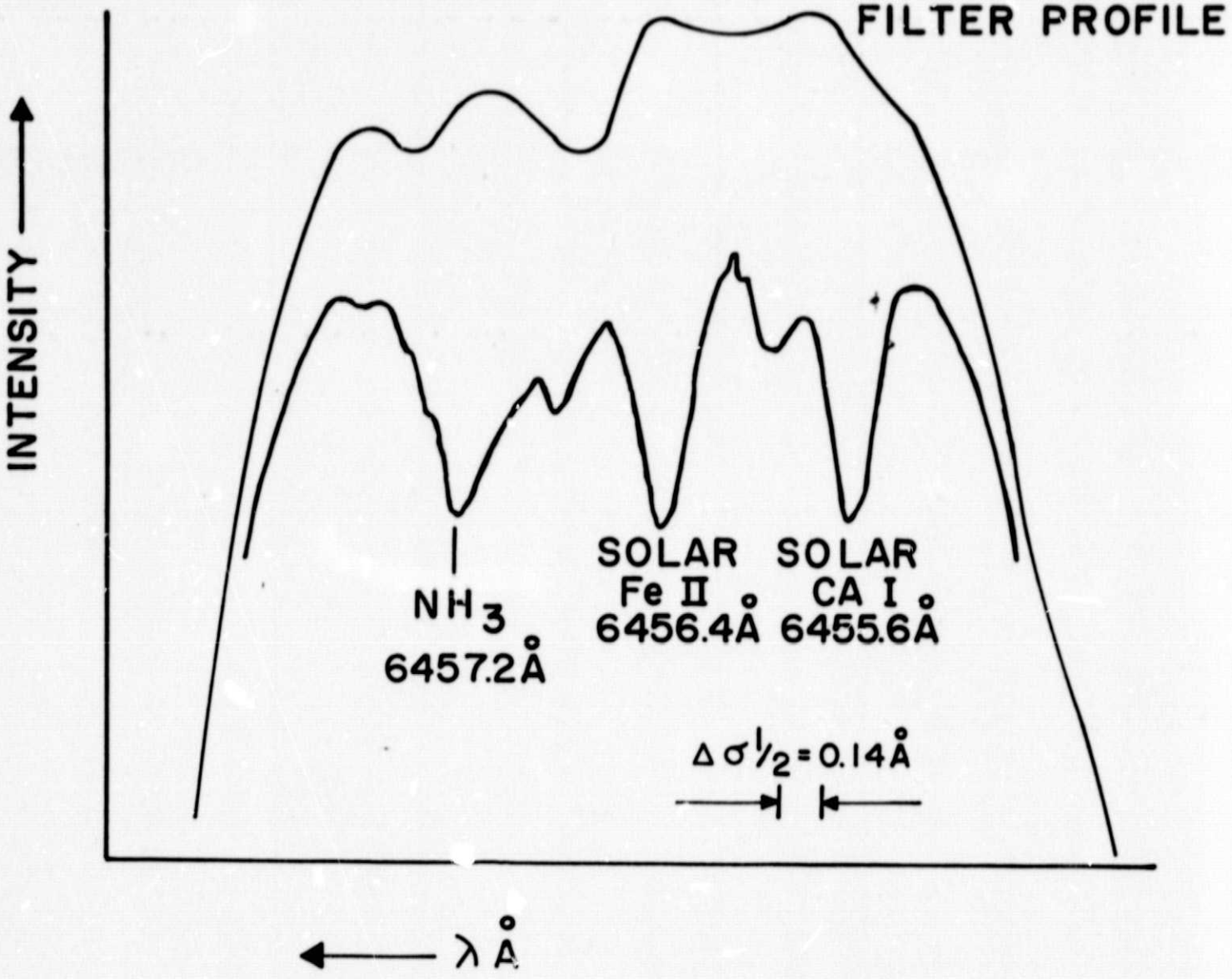
FILTER PROFILE
INTENSITY
SOLAR
Fe II
6456.4Å
SOLAR
CA I
6455.6Å
NH3
6457.2Å
Δσ1/2 = 0.14Å
λ Å